Supplemental Material on: Desynchronization transitions in adaptive networks

Rico Berner[1,2,*], Simon Vock[1], Eckehard Schöll[1,3,4], and Serhiy Yanchuk[2]

[1]Institut für Theoretische Physik, Technische Universität Berlin, Hardenbergstr. 36, 10623 Berlin, Germany
[2]Institut für Mathematik, Technische Universität Berlin, Straße des 17. Juni 136, 10623 Berlin, Germany
[3]Bernstein Center for Computational Neuroscience Berlin, Humboldt-Universität, Philippstraße 13, 10115 Berlin, Germany
[4]Potsdam Institute for Climate Impact Research, Telegrafenberg A 31, 14473 Potsdam, Germany

I. DERIVATION OF THE MASTER STABILITY FUNCTION FOR ADAPTIVE COMPLEX NETWORKS

In this section, we derive the master stability function for system (1)–(2) from the main text. For convenience, we repeat these equations here:

$$\dot{\boldsymbol{x}}_i = f(\boldsymbol{x}_i) - \sigma \sum_{j=1}^{N} a_{ij}\kappa_{ij} g(\boldsymbol{x}_i, \boldsymbol{x}_j), \tag{S1}$$

$$\dot{\kappa}_{ij} = -\epsilon \left(\kappa_{ij} + a_{ij} h(\boldsymbol{x}_i - \boldsymbol{x}_j)\right), \tag{S2}$$

where the adjacency matrix has constant row sum $r = \sum_{j=1}^{N} a_{ij}$.

Let $(\boldsymbol{s}(t), \kappa_{ij}^s)$ be the synchronous state, i.e., $\boldsymbol{x}_i = \boldsymbol{s}(t)$ and $\kappa_{ij} = \kappa_{ij}^s$ for all $i, j = 1\dots, N$. This state solves the set of differential Eqs. (3)–(4) of the main text.

In order to describe the local stability of the synchronous state, we derive the variational equation for small perturbations close to this state. For this, we introduce the following vector variables denoting the deviations from the synchronized state: $\boldsymbol{\xi} = \boldsymbol{x} - \mathbb{I}_N \otimes \boldsymbol{s}$, and $\boldsymbol{\chi} = \boldsymbol{\kappa} - \boldsymbol{\kappa}^s$ with

$$\boldsymbol{x} = (\boldsymbol{x}_1^T, \cdots, \boldsymbol{x}_N^T)^T,$$
$$\boldsymbol{\kappa} = (\kappa_{11}, \cdots, \kappa_{1N}, \kappa_{21}, \cdots, \kappa_{NN})^T,$$

where $\otimes$ denotes the Kronecker product. Using the following notations

$$\mathbf{a}_i = (a_{i1}, \dots, a_{iN}),$$
$$\mathrm{diag}(\mathbf{a}_i) = \begin{pmatrix} a_{i1} & & \\ & \ddots & \\ & & a_{iN} \end{pmatrix},$$

and the $N \times N^2$, $N^2 \times N$, and $N^2 \times N$ matrices

$$B = \begin{pmatrix} \mathbf{a}_1 & & \\ & \ddots & \\ & & \mathbf{a}_N \end{pmatrix},$$
$$C = B^T - D,$$
$$D = \begin{pmatrix} \mathrm{diag}(\mathbf{a}_1) \\ \vdots \\ \mathrm{diag}(\mathbf{a}_N) \end{pmatrix},$$

respectively, the variational equation reads

$$\begin{pmatrix} \dot{\boldsymbol{\xi}} \\ \dot{\boldsymbol{\chi}} \end{pmatrix} = \begin{pmatrix} S & -\sigma B \otimes g(\boldsymbol{s}, \boldsymbol{s}) \\ -\epsilon C \otimes \mathrm{D}h(0) & -\epsilon \mathbb{I}_{N^2} \end{pmatrix} \begin{pmatrix} \boldsymbol{\xi} \\ \boldsymbol{\chi} \end{pmatrix}, \tag{S3}$$

where

$$S = \mathbb{I}_N \otimes \mathrm{D}f(\boldsymbol{s}) + \sigma h(0) \left(r \mathbb{I}_N \otimes \mathrm{D}_1 g(\boldsymbol{s}, \boldsymbol{s}) + A \otimes \mathrm{D}_2 g(\boldsymbol{s}, \boldsymbol{s})\right).$$

We note that matrices B, C, and D satisfy the relations $B \cdot B^T = r\mathbb{I}_N$, $B \cdot D = A$, and $B \cdot C = L$, which can be obtained by straightforward calculation.

Due to the structure of the variational equation (S3), there exist $N^2 - N$ eigenvalues $\lambda = -\epsilon$. The corresponding time-independent eigenspace can be found from

$$\begin{pmatrix} S + \epsilon \mathbb{I}_{Nd} & -\sigma B \otimes g(\boldsymbol{s}, \boldsymbol{s}) \\ -\epsilon C \otimes \mathrm{D}h(0) & 0 \end{pmatrix} \begin{pmatrix} \boldsymbol{\xi} \\ \boldsymbol{\chi} \end{pmatrix} = 0.$$

One can see that $(\boldsymbol{\xi}, \boldsymbol{\chi})$ such that $\boldsymbol{\xi} = 0$ and $B\boldsymbol{\chi} = 0$ are the time-independent eigenvectors. Moreover, the relation $B\boldsymbol{\chi} = 0$ defines $N^2 - N$ linearly independent eigenvectors spanning the eigenspace corresponding to the eigenvalues $\lambda = -\epsilon$. This follows from the fact that $\boldsymbol{\chi}$ is N^2-dimensional and $\mathrm{rank}(B) = N$ if the row sum r of A is non-zero.

With these prerequisites we are now able to simplify the local stability analysis on adaptive networks and find a master stability function.

Let (S1)–(S2) *possess a synchronous solution* $(\boldsymbol{s}, \kappa_{ij}^s)$. *Further, let* (S3) *be the variational equations around this synchronous solution and assume that the Laplacian matrix L is diagonalizable. Then, the synchronous solution is locally stable if and only if for all eigenvalues $\mu \in \mathbb{C}$ of the Laplacian matrix, the largest Lyapunov exponent (if it exists), i.e., the master stability function $\Lambda(\mu)$, of the following system is negative*

$$\frac{\mathrm{d}\boldsymbol{\zeta}}{\mathrm{d}t} = \Big(\mathrm{D}f(\boldsymbol{s}) + \sigma r h(0)\big(\mathrm{D}_1 g(\boldsymbol{s}, \boldsymbol{s}) + (1 - \frac{\mu}{r})\mathrm{D}_2 g(\boldsymbol{s}, \boldsymbol{s})\big)\Big)\boldsymbol{\zeta} - \sigma g(\boldsymbol{s}, \boldsymbol{s})\kappa, \tag{S4}$$

$$\frac{\mathrm{d}\kappa}{\mathrm{d}t} = -\epsilon \left(\mu \mathrm{D}h(0)\boldsymbol{\zeta} + \kappa\right). \tag{S5}$$

Here, $\boldsymbol{\zeta} \in \mathbb{C}^d$ and $\kappa \in \mathbb{C}$.

In the following we present the derivation of (S4)–(S5). As it is shown above, there are N^2-N independent vectors $\boldsymbol{w}_l$ ($l=1,\dots,N^2-N$) spanning the kernel of B, i.e. $B\boldsymbol{w}_l=0$. Using the Gram-Schmidt procedure we find an orthonormal basis for $\ker(B)=\operatorname{span}\{\boldsymbol{v}_1,\dots,\boldsymbol{v}_{N^2-N}\}$. With this, we define the $N^2\times(N^2-N)$ matrix $Q=(\boldsymbol{v}_1,\dots,\boldsymbol{v}_{N^2-N})$. Consider now the $(N^2+Nd)\times(N^2+Nd)$ matrix

$$R=\begin{pmatrix}\mathbb{I}_{Nd} & 0 & 0\\ 0 & (1/r)B^T & Q\end{pmatrix}$$

with left inverse

$$R^{-1}=\begin{pmatrix}\mathbb{I}_{Nd} & 0\\ 0 & B\\ 0 & Q^T\end{pmatrix},$$

i.e., $R^{-1}R=\mathbb{I}_{N^2+Nd}$. Introduce the new coordinates given by $R\begin{pmatrix}\boldsymbol{\xi}\\ \hat{\boldsymbol{\chi}}\end{pmatrix}=\begin{pmatrix}\boldsymbol{\xi}\\ \boldsymbol{\chi}\end{pmatrix}$ for which the variational equation then reads

$$\frac{\mathrm{d}}{\mathrm{d}t}\begin{pmatrix}\boldsymbol{\xi}\\ \hat{\boldsymbol{\chi}}\end{pmatrix}=R^{-1}\begin{pmatrix}S & -\sigma B\otimes g(\boldsymbol{s},\boldsymbol{s})\\ -\epsilon C\otimes \mathrm{D}h(0) & -\epsilon\mathbb{I}_{N^2}\end{pmatrix}R\begin{pmatrix}\boldsymbol{\xi}\\ \hat{\boldsymbol{\chi}}\end{pmatrix}.$$

We further obtain

$$\begin{aligned}R^{-1}&\begin{pmatrix}S & -\sigma B\otimes g(\boldsymbol{s},\boldsymbol{s})\\ -\epsilon C\otimes \mathrm{D}h(0) & -\epsilon\mathbb{I}_{N^2}\end{pmatrix}R\\ &=R^{-1}\begin{pmatrix}S & -\sigma\mathbb{I}_N\otimes g(\boldsymbol{s},\boldsymbol{s}) & 0\\ -\epsilon C\otimes \mathrm{D}h(0) & -\epsilon/rB^T & -\epsilon Q\end{pmatrix}\\ &=\begin{pmatrix}S & -\sigma\mathbb{I}_N\otimes g(\boldsymbol{s},\boldsymbol{s}) & 0\\ -\epsilon L\otimes \mathrm{D}h(0) & -\epsilon\mathbb{I}_N & 0\\ -\epsilon Q^TC\otimes \mathrm{D}h(0) & 0 & -\epsilon\mathbb{I}_{N^2-N}\end{pmatrix}.\end{aligned}$$

These equations yield that there are $Nd+N$ coupled differential equations left

$$\frac{\mathrm{d}}{\mathrm{d}t}\begin{pmatrix}\boldsymbol{\xi}\\ \boldsymbol{\chi}_M\end{pmatrix}=\begin{pmatrix}S & -\sigma\mathbb{I}_N\otimes g(\boldsymbol{s},\boldsymbol{s})\\ -\epsilon L\otimes \mathrm{D}h(0) & -\epsilon\mathbb{I}_N\end{pmatrix}\begin{pmatrix}\boldsymbol{\xi}\\ \boldsymbol{\chi}_M\end{pmatrix}\tag{S6}$$

with $\boldsymbol{\chi}_M=\hat{\boldsymbol{\chi}}_1$ that determine the stability for the synchronous state, and N^2-N slave equations

$$\frac{\mathrm{d}}{\mathrm{d}t}\boldsymbol{\chi}_S=\begin{pmatrix}-\epsilon Q^TC\otimes\mathrm{D}h(0) & 0 & -\epsilon\mathbb{I}_{N^2-N}\end{pmatrix}\begin{pmatrix}\boldsymbol{\xi}\\ \boldsymbol{\chi}_M\\ \boldsymbol{\chi}_S\end{pmatrix}$$

with $\boldsymbol{\chi}_S=(\hat{\boldsymbol{\chi}}_2^T,\dots,\hat{\boldsymbol{\chi}}_N^T)^T$ which are driven by the variables $\boldsymbol{\xi}$ and, hence, can be solved explicitly once the latter once are known. By assumption, there is a unitary matrix $D_L=U^HLU$ where D_L is the diagonalization of the Laplacian matrix L. Transforming the differential equation (S6) by using the unitary transformation U, we get

$$\frac{\mathrm{d}}{\mathrm{d}t}\begin{pmatrix}\boldsymbol{\zeta}\\ \boldsymbol{\kappa}\end{pmatrix}=\begin{pmatrix}\mathbb{I}_N\otimes Df(\boldsymbol{s})+\sigma h(0)\left(r\mathbb{I}_N\otimes\mathrm{D}_1g(\boldsymbol{s},\boldsymbol{s})+(r\mathbb{I}_N-D_L)\otimes\mathrm{D}_2g(\boldsymbol{s},\boldsymbol{s})\right) & -\sigma\mathbb{I}_N\otimes g(\boldsymbol{s},\boldsymbol{s})\\ -\epsilon D_L\otimes\mathrm{D}h(0) & -\epsilon\mathbb{I}_N\end{pmatrix}\begin{pmatrix}\boldsymbol{\zeta}\\ \boldsymbol{\kappa}\end{pmatrix}$$

where $\begin{pmatrix}U\otimes\mathbb{I}_d & 0\\ 0 & U\end{pmatrix}\begin{pmatrix}\boldsymbol{\xi}\\ \boldsymbol{\chi}_M\end{pmatrix}=\begin{pmatrix}\boldsymbol{\zeta}\\ \boldsymbol{\kappa}\end{pmatrix}$.

Remarkably, the master stability function Λ depends explicitly on the row sum r. Moreover, the master stability function seems to depend on σ, r, and μ independently. The time scale separation parameter ϵ is always kept fixed. However, in any case, one parameter can be disregarded. To see this, we note that the solution to the Eq. (S5) is explicitly solvable and the solution reads

$$\kappa=\kappa_0e^{-\epsilon(t-t_0)}-\epsilon\mu\mathrm{D}h(0)\int_{t_0}^{t}e^{-\epsilon(t-t')}\zeta(t')\,dt',$$

where the first term vanishes for $t\to\infty$ and hence can be neglected (when studying asymptotic stability for $t\to\infty$). We use this and rewrite the asymptotic dynamics of (S4)–(S5) in its integro-differential form

$$\begin{aligned}\frac{\mathrm{d}\boldsymbol{\zeta}}{\mathrm{d}t}=&\Big(\mathrm{D}f(\boldsymbol{s})+\sigma rh(0)\Big(\mathrm{D}_1g(\boldsymbol{s},\boldsymbol{s})\\ &+(1-\frac{\mu}{r})\mathrm{D}_2g(\boldsymbol{s},\boldsymbol{s})\Big)\Big)\boldsymbol{\zeta}\\ &+\epsilon\sigma r\frac{\mu}{r}g(\boldsymbol{s},\boldsymbol{s})\mathrm{D}h(0)\int_{t_0}^{t}e^{-\epsilon(t-t')}\boldsymbol{\zeta}(t')\,dt'.\end{aligned}\tag{S7}$$

Hence, the master stability function can be regarded as a function of two parameters, i.e., $\Lambda(\sigma,\mu,r)=\Lambda(\sigma r,\mu/r)$. Furthermore, in case of diffusive coupling, i.e., $g(\boldsymbol{x},\boldsymbol{y})=g(\boldsymbol{x}-\boldsymbol{y})$, the master stability function can be regarded as a function of only one parameter $\Lambda(\sigma,\mu,r)=\Lambda(\sigma\mu)$. This is due to the fact that $\mathrm{D}_1 g(\boldsymbol{s},\boldsymbol{s}) = \mathrm{D}_1 g(0) = -\mathrm{D}_2 g(0)$ and hence the dependency on r vanishes in Eq. (S7).

II. MASTER STABILITY FUNCTION FOR ADAPTIVE PHASE OSCILLATOR NETWORKS

In this section, we provide a brief analysis of the master stability function for the adaptive Kuramoto-Sakaguchi network (9)–(10) of the main text. Using the result of Section I, the stability of the synchronous state of system (9)–(10) of the main text is governed by the two differential equations

$$\frac{\mathrm{d}}{\mathrm{d}t}\begin{pmatrix}\zeta\\ \kappa\end{pmatrix} = \begin{pmatrix}\mu\sigma\cos(\alpha)\sin(\beta) & -\sigma\sin(\alpha)\\ -\epsilon\mu\cos(\beta) & -\epsilon\end{pmatrix}\begin{pmatrix}\zeta\\ \kappa\end{pmatrix},$$

where $\mu\in\mathbb{C}$ stands for all eigenvalues of the Laplacian matrix L corresponding to the base network described by the adjacency matrix A. The characteristic polynomial in λ of the latter system is of degree two and reads

$$\lambda^2 + (\epsilon - \sigma\mu\cos(\alpha)\sin(\beta))\,\lambda - \epsilon\sigma\mu\sin(\alpha+\beta) = 0. \tag{S8}$$

The master stability function is given as $\Lambda(\sigma\mu) = \max(\mathrm{Re}(\lambda_1), \mathrm{Re}(\lambda_2))$ where λ_1 and λ_2 are the two solutions of the quadratic polynomial (S8). Figure 1 of the main text displays the master stability function for different parameters.

The boundary of the region in $\sigma\mu$ parameter space that corresponds to stable local dynamics, is given by $\lambda = \mathrm{i}\gamma$ with $\gamma\in\mathbb{R}$. Plugging this into Eq. (11) of the main text, we obtain

$$\sigma\mu = Z(\gamma) = a(\gamma) + \mathrm{i}b(\gamma)$$

with

$$a(\gamma) = \epsilon\frac{\gamma^2\left(\cos\alpha\sin\beta - \sin(\alpha+\beta)\right)}{\gamma^2\cos^2\alpha\sin^2\beta + \epsilon^2\sin^2(\alpha+\beta)},$$
$$b(\gamma) = \frac{\gamma^3\cos\alpha\sin\beta + \epsilon^2\gamma\sin(\alpha+\beta)}{\gamma^2\cos^2\alpha\sin^2\beta + \epsilon^2\sin^2(\alpha+\beta)}.$$

Due to the symmetry of the master stability function, a necessary condition to observe a stability island is that the curve $\sigma\mu(\gamma)$ possesses two crossings with the real axis, i.e., two real solutions for $b(\gamma)=0$. The three crossings are given by $\gamma_1 = 0$ and as real solutions γ_2 and γ_3 of $\gamma^2\cos\alpha\sin\beta = -\epsilon^2\sin(\alpha+\beta)$. From this we deduce the existence condition for stability islands: $\sin(\alpha+\beta)/(\cos\alpha\sin\beta) < 0$ ($\epsilon > 0$). Note that $a(\gamma_2) = a(\gamma_3)$.

III. THE CLUSTER PARAMETER

In this section, we introduce the cluster parameter R_C as a measure for coherence in a system of coupled phase oscillators. A measure that can be used in order to detect frequency synchronization between two oscillators relies on the mean phase velocity (average frequency) of each phase oscillator

$$\Omega_i = \lim_{T\to\infty}\frac{1}{T}\left(\phi_i(t_0+T) - \phi_i(t_0)\right). \tag{S9}$$

The frequency synchronization measure between nodes is given by

$$\Omega_{ij} = \begin{cases}1, \text{if } \Omega_i - \Omega_j = 0,\\ 0, \text{otherwise.}\end{cases} \tag{S10}$$

Numerically the limit is approximated by a very long averaging window. In addition, we use a sufficiently small threshold ϖ in order to detect frequency synchronization numerically, i.e., $\Omega_{ij} = 1$ if $\Omega_i - \Omega_j < \varpi$. For the analysis presented here and in the main text, we use $\varpi = 0.001$. Using the measure Ω_{ij}, we define the cluster parameter

$$R_C = \frac{1}{N^2}\sum_{i,j=1}^{N}\Omega_{ij}. \tag{S11}$$

The cluster parameter measures the following. First, for each frequency cluster, the total number of pairwise synchronized nodes is computed. Second, all pairs of two nodes from the same cluster are summed up and normalized by the number of all possible pairs of nodes N^2. In case of full synchronization, frequency clustering, or incoherence the values of the cluster parameter are $R_C = 1$, $1 < R_C < 0$, or $R_C = 0$, respectively. A similar measure can be found in Refs. [1, 2].

IV. DESYNCHRONIZATION TRANSITION AND THE FORMATION OF PARTIAL SYNCHRONIZATION PATTERNS IN ADAPTIVE PHASE OSCILLATOR NETWORKS

In this section, we provide further details on the desynchronization transition in a network of adaptively coupled phase oscillators (9)–(10).

Figure S1 shows the cluster parameter R_C for different values of the coupling constant σ. In the adiabatic continuation, we increase σ step-wise after an integration time of $t = 10000$. For each simulation, the final state of the previous simulations is taken as the initial condition with an additional small perturbation. Note that $R_C = 1$ refers to full in-phase synchrony of the oscillators. We observe that, for small σ, the synchronous state is stable, see Fig. S1(d,g,j). Here, the stability of the synchronous state is directly implied by the master stability

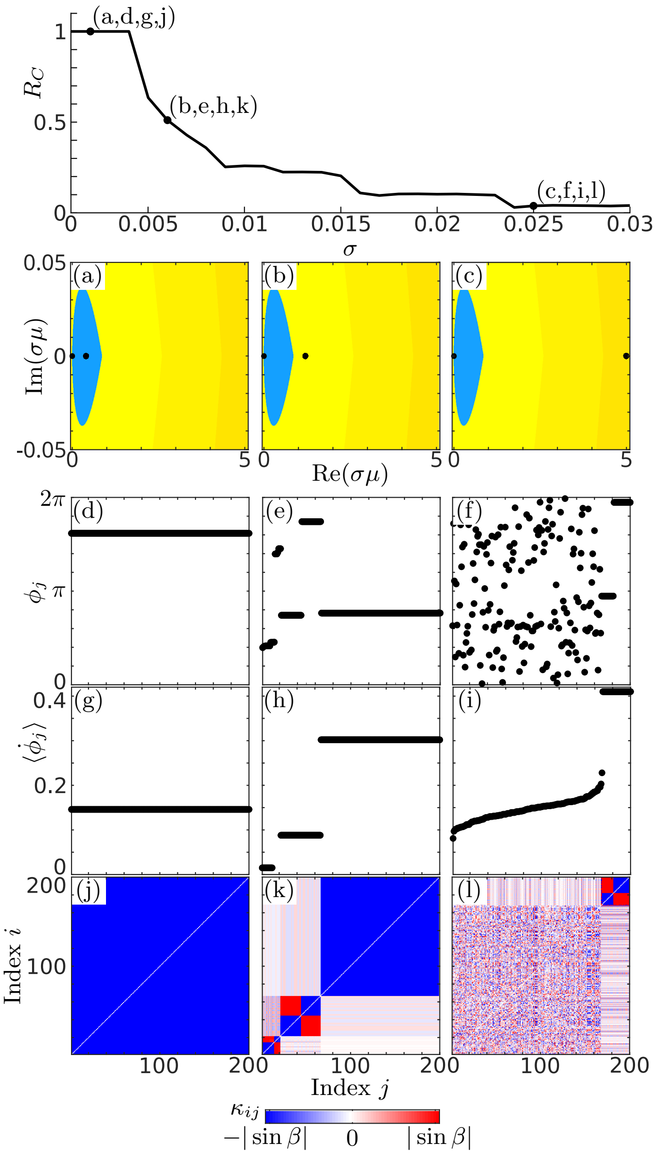

FIG. S1. Dynamics in a globally coupled network of 200 phase oscillators Eqs. (9)–(10) of the main text for different values of overall coupling strength σ than in Fig.2 of the main text. Adiabatic continuation for increasing σ with the stepsize of 0.001, starting with the synchronous state $\phi_i = 0$, $\kappa_{ij} = -a_{ij}\sin\beta$. The top panel shows the cluster parameter R_C vs σ. For the three values of σ: (a,d,g,j) $\sigma = 0.002$, (b,e,h,k) $\sigma = 0.006$, and (c,f,i,l) $\sigma = 0.025$, the plots show: in (a,b,c) the master stability function (color coded as in Fig. 1 of the main text), together with $\sigma\mu_i$, where μ_i are the N Laplacian eigenvalues of A; in (d,e,f) snapshots for ϕ_i at $t = 30000$; in (g,h,i) the temporal average of the phase velocities $\langle\dot{\phi}_i\rangle$ over the last 5000 time units; and in (j,k,l) snapshots for the coupling matrix κ_{ij} at $t = 30000$. Other parameters: $\alpha = 0.49\pi$, $\beta = 0.88\pi$, $\epsilon = 0.01$.

function. We note that all Laplacian eigenvalues μ_i of a globally coupled network are given by either $\mu_i = 0$ or $\mu_i = N$. In Figure S1(a), all master function parameters $\sigma\mu$ lie within the stability island.

By increasing the coupling constant, the values $\sigma\mu_i$ move out of the stability regions and the synchronous state becomes unstable. For intermediate values of σ the emergence of multiclusters with hierarchical structure in the cluster size are observed. In Figure S1(e,h,k) a multicluster states is shown with three clusters. Note that for the system (9)–(10) of the main text, in-phase synchronous and antipodal clusters have the same properties [3, 4]. In Refs. [3, 4] the role of the hierarchical structure of the cluster sizes have been discussed. Increasing the coupling constant further shows the emergence of incoherence. In Figure S1(f,i,l), we show the coexistence of a coherent and an incoherent cluster. These states, also called chimera-like states, have been numerically analyzed in Refs. [1, 2, 5].

V. NETWORK OF COUPLED FITZHUGH-NAGUMO NEURONS WITH SYNAPTIC PLASTICITY

In this section, we describe the model of coupled FitzHugh-Nagumo neurons with synaptic plasticity and present the synchronous state used in the main text. The model is given by

$$\tau\dot{u}_i = u_i - \frac{u_i^3}{3} - v_i - \sigma\sum_{j=1}^{N} a_{ij}\kappa_{ij}u_i I_j, \tag{S12}$$

$$\dot{v}_i = u_i + a - bv_i, \tag{S13}$$

$$\dot{I}_i = \alpha(u_i)(1 - I_i) - I_i/\tau_{\mathrm{syn}}, \tag{S14}$$

$$\dot{\kappa}_{ij} = -\epsilon\left(\kappa_{ij} + a_{ij}e^{-\beta_1(u_i-u_j+\beta_2)^2}\right). \tag{S15}$$

Here u_i denotes the membrane potential and v_i summarizes the recovery processes for each neuron; I_i describes the synaptic output for each neuron; the parameters $a = 0.7$ and $b = 0.2$ are fixed to the values corresponding to self-sustained oscillatory dynamics of uncoupled neurons; and $\tau = 0.08$ and $\epsilon = 0.01$ are fixed time scale separation parameters between the fast activation and slow inhibitory processes in each neuron, and between the fast oscillatory dynamics and the slow adaptation of the coupling weights, respectively. The synaptic recovery function is given by $\alpha(u) = 2/(0.08(1 + \exp(-u/0.05)))$. The synaptic timescale is $\tau_{\mathrm{syn}} = 5/6$. All variables and parameters are summarized in Tab. S1. The form of the synaptic plasticity is similar to the rules used in [6, 7]. We introduce β_1 and β_2 as control parameters. In particular, we have $\beta_1 = -h(0)/(2\mathrm{D}h(0)\beta_2)$ and $\beta_2 = (2\mathrm{D}h(0)_1 \ln(\mathrm{D}h(0)_1))/h(0)$ where $\mathrm{D}h(0)_1$ denotes the first component of $\mathrm{D}h(0)$.

The synchronous state of the equations (S12)–(S15) is

u_i	membrane potential/activator
v_i	recovery/inhibitor variable
I_i	synaptic output variable
κ_{ij}	variable coupling weights
N	number of oscillators
a_{ij}	entries of adjacency matrix, $a_{ij} \in \{0, 1\}$
σ	overall coupling strength
r	row sum, i.e., $r = \sum_{j=1}^{N} a_{ij}$
$a = 0.7, b = 0.2$	bifurcation parameters of the FitzHugh-Nagumo neuron
$\tau = 0.08$	controls time separation between fast activation and slow inhibition
$\epsilon = 0.01$	controls time separation between fast oscillation and slow adaptation
$\tau_{\mathrm{syn}} = 5/6$	synaptic decay rate
$u_{\mathrm{shp}} = 0.05$	coupling shape parameter
β_1, β_2	adaption control parameters

TABLE S1. The table provides the meaning for each variable and parameter used in (S12)–(S15).

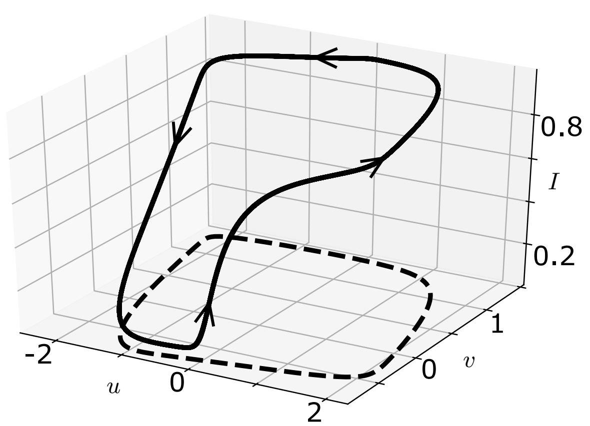

FIG. S2. Limit cycle in Eqs. (S16)–(S18) as solid line and the projection onto the u-v-plane as dashed line. Parameters: $\sigma = 0.002$, $r = 200$, $h(0) = 0.8$ and $\mathrm{D}h(0) = (80, 0, 0)$. All other parameters as in Tab. S1.

given by a solution of

$$\tau \dot{u}_s = u_s - \frac{u_i^3}{3} - v_s + \sigma r u_s I_s e^{-\beta_1 \beta_2^2}, \tag{S16}$$

$$\dot{v}_s = u_s + a - b v_s, \tag{S17}$$

$$\dot{I}_s = \alpha(u_s)(1 - I_s) - I_s/\tau_{\mathrm{syn}}, \tag{S18}$$

$$\kappa_{ij}^s = -a_{ij} e^{-\beta_1 \beta_2^2}, \tag{S19}$$

where $(u_i, v_i, I_i) = \boldsymbol{s} = (u_s, v_s, I_s)$ for all $i = 1, \ldots, N$. In Fig. S2, we display a limit cycle as a stable numerical solution of (S16)–(S19) for the set of parameters used in the main text.

VI. THE MASTER STABILITY FUNCTION AND DESYNCHRONIZATION TRANSITION IN ADAPTIVE NETWORKS OF FITZHUGH-NAGUMO NEURONS

In this section, we consider the model of adaptively coupled FitzHugh-Nagumo neurons (S12)–(S15). We give insights into the derivation of the system's master stability function as well as on the desynchronization transition induced by the adaptivity.

In order to investigate the local stability of the synchronous states that solves Eqs. (S16)–(S19), see Fig. S2, we linearize Eqs. (S12)–(S15) around these states. Using the results of Section I, the stability of the synchronous solution is governed by the set of equations

$$\begin{aligned}
\frac{\mathrm{d}\boldsymbol{\zeta}}{\mathrm{d}t} &= \Big(\mathrm{D}f(\boldsymbol{s}) + \sigma r h(0)\big(\mathrm{D}_1 g(\boldsymbol{s}, \boldsymbol{s}) \\
&\qquad + (1 - \frac{\mu}{r})\mathrm{D}_2 g(\boldsymbol{s}, \boldsymbol{s})\big)\Big)\boldsymbol{\zeta} - \sigma g(\boldsymbol{s}, \boldsymbol{s})\kappa, \\
\frac{\mathrm{d}\kappa}{\mathrm{d}t} &= -\epsilon\left(\mu \mathrm{D}h(0)\boldsymbol{\zeta} + \kappa\right).
\end{aligned}$$

Here, the derivatives of the functions f, g, and h are

$$\begin{aligned}
\mathrm{D}f(\boldsymbol{s}) &= \begin{pmatrix} \frac{1}{\tau}\left(1 - u_s^2\right) & -\frac{1}{\tau} & 0 \\ 1 & -b & 0 \\ \frac{\tau(\alpha(u_s))^2(1 - I_s)}{\alpha_0 u_{\mathrm{shp}} \exp(\frac{u_s}{u_{\mathrm{shp}}})} & 0 & -\alpha(u_s) - \frac{1}{\tau_{\mathrm{syn}}} \end{pmatrix}, \\
\mathrm{D}_1 g(\boldsymbol{s}, \boldsymbol{s}) &= \begin{pmatrix} I_s & 0 & 0 \\ 0 & 0 & 0 \\ 0 & 0 & 0 \end{pmatrix}, \\
\mathrm{D}_2 g(\boldsymbol{s}, \boldsymbol{s}) &= \begin{pmatrix} 0 & 0 & u_s \\ 0 & 0 & 0 \\ 0 & 0 & 0 \end{pmatrix}, \\
\mathrm{D}h(0) &= \begin{pmatrix} -2\beta_1\beta_2 \exp(-\beta_1\beta_2^2) & 0 & 0 \end{pmatrix}.
\end{aligned}$$

Using this, we are able to determine numerically the maximum Lyapunov exponents and hence the stability of the periodic orbit displayed in Fig. S2. In Fig. S3, we show different shapes of the master stability function depending on the form of the plasticity rule, i.e., depending on $h(0)$ and $\mathrm{D}h(0)$. We observe that for certain parameters almost complete half spaces in the μ/r-plane refer to stable or unstable local dynamics, see Fig. S3(a,b). This is similar to Fig. 1(d,e) of the main text where we display the master stability function of the phase oscillator model. Most remarkably, similar to the phase oscillator model (9)–(10) we find parameters for which stability islands exist, see Fig. S3(d).

As we know from the example of phase oscillators, the presence of a stability island may induce a desynchronization transition for an increasing overall coupling strength σ. In order to show this transition, we follow the same approach already presented in Fig. S1. The results of the adiabatic continuation on a globally coupled network

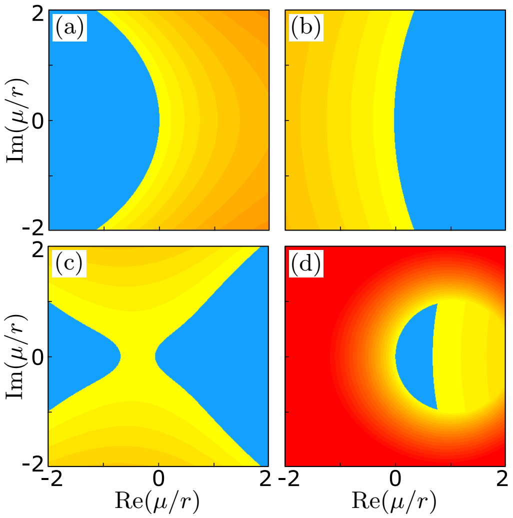

FIG. S3. The master stability functions for the synchronous solution of (S12)–(S15) and different plasticity rules are displayed (color code as in Fig. 1 of the main text). Regions belonging to negative Lyapunov exponents are colored blue. Parameters: the control parameters β_1 and β_2 are chosen such that (a) $h(0) = 0.8$, D$h(0) = (50, 0, 0)$ (b) $h(0) = -0.2$, D$h(0) = (0, 0, 0)$, (c) $h(0) = 0.8$, D$h(0) = (10, 0, 0)$, and (d) $h(0) = 0.4$, D$h(0) = (50, 0, 0)$. The overall coupling constant is set to $\sigma = 0.005$. All other parameters are as in Fig. S2.

are shown in Fig. S4. We note that in contrast to the case of phase oscillators, here, the shape of the master stability function depends explicitly on σ. The desynchronization is described in the main text. Additionally to the figure given in the main text, we provide plots for the coupling matrices in Fig. S4(j,k,l). The coupling matrices show very nicely the emergence of partial synchronization structures in the transition from coherence to incoherence which is induced by the stability island.

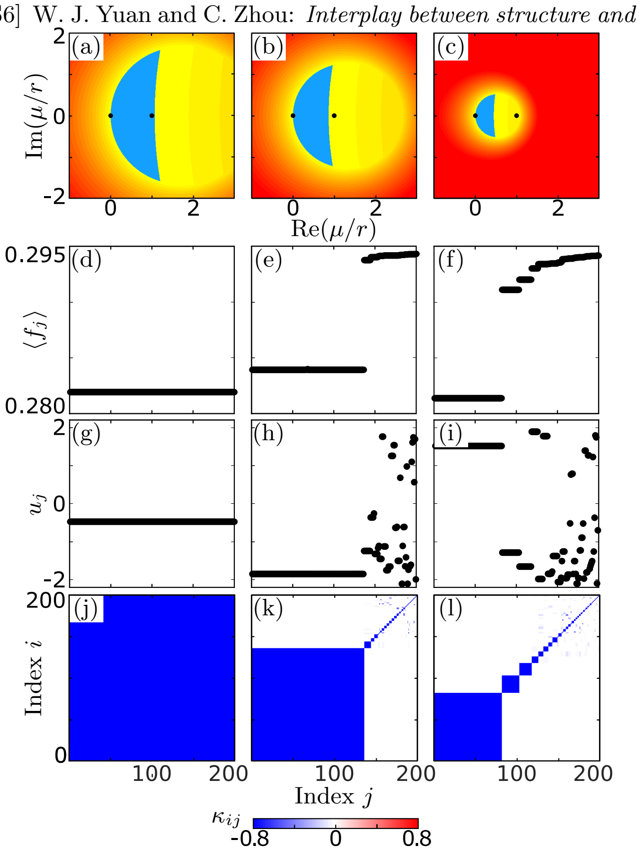

FIG. S4. Dynamics of globally coupled network of 200 FitzHugh-Nagumo neurons with plasticity Eqs. (S12)–(S15). Adiabatic continuation for an increasing overall coupling strength σ with the step size 0.0005, starting with the synchronous state of Eqs. (S12)–(S15). For the three values of σ: (a,d,g,j) $\sigma = 0.002$, (b,e,h,k) $\sigma = 0.0025$, and (c,f,i,l) $\sigma = 0.005$, the plots show: in (a,b,c), the master stability function, together with μ_i/r, where μ_i are the N Laplacian eigenvalues (color code as in Fig. 1 of the main text), in (d,e,f) the average frequency $\langle f_i \rangle$, in (g,h,i) snapshots for u_i at $t = 10000$, and in (j,k,l) snapshots for the coupling matrices κ_{ij} at $t = 10000$. Here $\langle f_i \rangle = M_i/1000$, where M_i is the number of rotations (spikes) of neuron i during the time interval of length 1000. The control parameters for the adaptation rule β_1 and β_2 are chosen such that $h(0) = 0.8$ and D$h(0) = (80, 0, 0)$. All other parameters can be taken from Tab. S1.

[S1] D. V. Kasatkin, S. Yanchuk, E. Schöll, and V. I. Nekorkin: *Self-organized emergence of multi-layer structure and chimera states in dynamical networks with adaptive couplings*, Phys. Rev. E **96**, 062211 (2017).

[S2] D. V. Kasatkin and V. I. Nekorkin: *The effect of topology on organization of synchronous behavior in dynamical networks with adaptive couplings*, Eur. Phys. J. Spec. Top. **227**, 1051 (2018).

[S3] R. Berner, E. Schöll, and S. Yanchuk: *Multiclusters in networks of adaptively coupled phase oscillators*, SIAM J. Appl. Dyn. Syst. **18**, 2227 (2019).

[S4] R. Berner, J. Fialkowski, D. V. Kasatkin, V. I. Nekorkin, S. Yanchuk, and E. Schöll: *Hierarchical frequency clusters in adaptive networks of phase oscillators*, Chaos **29**, 103134 (2019).

[S5] D. V. Kasatkin and V. I. Nekorkin: *Synchronization of chimera states in a multiplex system of phase oscillators with adaptive couplings*, Chaos **28**, 093115 (2018).

[S6] W. J. Yuan and C. Zhou: *Interplay between structure and dynamics in adaptive complex networks: Emergence and amplification of modularity by adaptive dynamics*, Phys. Rev. E **84**, 016116 (2011).

[S7] S. Chakravartula, P. Indic, B. Sundaram, and T. Killingback: *Emergence of local synchronization in neuronal networks with adaptive couplings*, PLoS ONE **12**, e0178975 (2017).

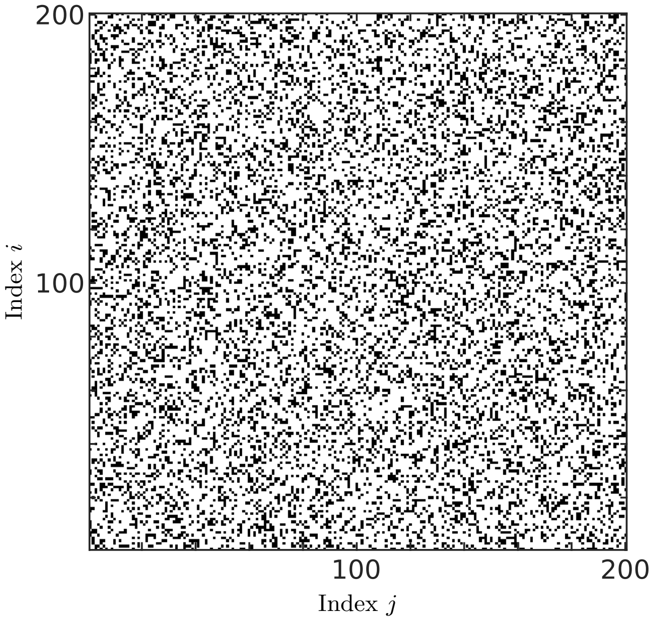

FIG. S5. Adjacency matrix A_c of a connected, directed random network of $N = 200$ nodes with constant row sum $r = 50$. The illustration shows the adjacency matrix where black and white refer to whether a link between two nodes exist or not, respectively.